

Analysis of Friction-Induced Oscillation in Negative Stiffness Control System

M. M. Zaglul Shahadat*, Takeshi Mizuno*, Yuji Ishino* and Masaya Takasaki*

*Department of Mechanical Engineering, Saitama University, 255 Shimo-Okubo, Saitama 338-8570, Japan
(Tel: 81-48-858-3453; e-mail: shahadat230@yahoo.com)

Abstract—The effect of friction on a negative stiffness control system is investigated. The series combination of isolators of negative and positive stiffness of equal magnitude provides infinite stiffness as well as zero compliance of the vibration isolation table against direct static load. However the performance of negative stiffness control system is affected by friction adversely. In another word, nonlinear friction causes an adverse effect to the negative stiffness control system, such as limit cycle. In the present work, the friction induced limit cycle of the negative stiffness control system is identified by using describing function method. The intersection of linear and nonlinear part of the control system in the same complex plane reveals the existence of limit cycle which varies according to the control parameters. Hence the relationship between the stiffness of the negative stiffness control system and induced limit cycle (frequency and amplitude) is established theoretically. The induced limit cycle behavior is determined by the conditions of nonlinear part at the points of intersection. Finally the theoretical limit cycle for a specific set of control parameters in designing the controller is verified by experimental result under the same conditions.

I. INTRODUCTION

IN many high-precision manufacturing and measuring process, position accuracy is a key performance objective. During the last three decades, accuracy requirements have turned into from micrometer range to the submicron and even nanometer range. Thus the precision vibration isolation plays an important role to meet the current demand of position accuracy in Hi-tech production processes. There are two main sources of vibration; (i) ground vibration and (ii) direct disturbance, which should be isolated from vibration free platform simultaneously. The zero stiffness and infinite stiffness are respectively ideal for reducing ground vibration and direct disturbance [1].

The infinite stiffness as well as zero compliance of vibration isolation is realized by connecting normal spring with magnetic suspension in series [2]. Zero-power magnetic suspension system has itself unique characteristic that it behaves as if it has negative stiffness. The linear actuator with proper controller of negative stiffness also causes the accomplishment of negative stiffness. The series combination of the negative stiffness actuator and the normal spring of equal magnitude provide infinite stiffness in a vertical system [3]. The principle of such vibration isolation has been applied to a developed horizontal vibration isolation system where

linear actuators are used to acquire both negative stiffness and positive stiffness [4].

The developed horizontal vibration isolation system is supported by four vertical supports of free bearing. In consequence, the developed active system is subjected to friction in contact areas. It is observed that the inherent friction leads to a sustained oscillation or limit cycle in the negative stiffness control system whereas such oscillation has not been observed for positive stiffness control in the same system. The phenomenon of oscillation due to friction is often unexpected as it causes additional dynamic loads, as well as faulty operation of machines and devices. Moreover, the presence of friction induced nonlinearity often affects the performance of active system adversely [5]. There are several methods to analyze the friction nonlinearity; the describing function method is exploited and a relationship between the magnitude of negative stiffness and the induced limit cycle is established in this paper.

II. VIBRATION ISOLATION WITH NEGATIVE STIFFNESS CONTROLLER

A. Realizing of infinite stiffness using negative stiffness

To acquire a high-performance vibration isolation system, the control system should be stiff against direct disturbance and should be soft suspension against ground vibration. This behavior has been achieved by using the concept of series connection of negative stiffness and positive stiffness of same magnitude [2]-[4].

When two isolators having stiffness coefficients k_1 and k_2 connected in series as shown in Fig. 1, then the combined stiffness k_c becomes as follows

$$k_c = \frac{k_1 k_2}{k_1 + k_2} \quad (1)$$

It shows that the combined stiffness of two series connected isolators is lower than that of each isolator. However if one isolator has negative stiffness and satisfies the following condition

$$k_1 = -k_2, \quad (2)$$

then the resultant combined stiffness of the corresponding isolators becomes infinite as follows,

$$k_c = \frac{(-k_2)k_2}{-k_2 + k_2} = \infty. \quad (3)$$

B. Active suspension

Horizontal suspension systems with conventional passive isolator are subjected to dislocation into downward when they work on inclined plane. Since self-dislocation can be treated as direct disturbance, thus the concept of negative stiffness as well as infinite stiffness (mentioned in II-A) could be applied to horizontal suspension system to hold the position of itself on inclined surface.

Moreover, if an inclined system is isolated from ground by high stiffness isolator, then there will be no dislocation but the ground vibration would transmit to the suspended object directly without attenuation. To overcome such problem, the middle mass with soft stiffness is added at the base portion of the horizontal suspension system shown in Fig. 2.

III. DESIGN OF STIFFNESS CONTROL

In this section, the designing of controllers for realizing negative stiffness and positive stiffness with linear actuator (voice coil motor (VCM)) are addressed. A basic single degree-of-freedom model of vibration isolation table with linear actuator (VCM) for designing the controllers is shown in Fig. 3. It is assumed that the moving table with mass m moves along horizontal translation (x -axis) without any internal interference of other axes motion. The motion equation of the table actuated by VCM is given in below

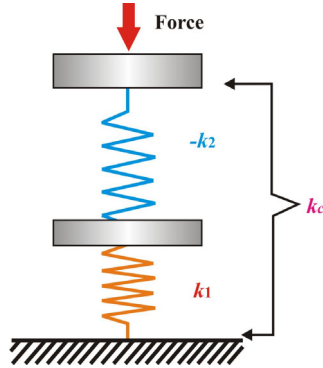


Fig. 1. Series connected springs

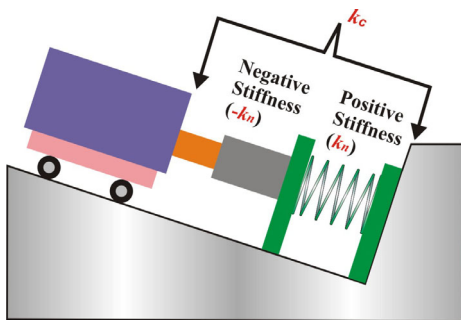


Fig. 2. Cancellation of dislocation with infinite stiffness

$$m\ddot{x} = f_a + f_d, \quad (4)$$

where

x : relative displacement of the table,

f_a : actuator's thrust force,

f_d : direct disturbance acting on the table.

The thrust exerted by the actuator is proportional to the coil current i , so the force f_a can be expressed as

$$f_a = k_i i, \quad (5)$$

where

k_i : actuator thrust force coefficient.

The Laplace-transforms of the Eqs. (4) and (5) give transfer function representation of actuator's dynamics written as

$$X(s) = \frac{1}{s^2} (b_0 I(s) + d_0 F_d(s)), \quad (6)$$

where each Laplace-transformed variable is denoted by its capital and

$$b_0 = \frac{k_i}{m}, \quad d_0 = \frac{1}{m}.$$

The feedback control current to the actuator correspond to linear control law usually is expressed by

$$G_n(s) = \frac{I(s)}{X(s)} = -\frac{h(s)}{g(s)}. \quad (7)$$

If the transfer function of the controller is strictly proper, then the polynomials can be represented as

$$g(s) = s^n + \sum_{k=0}^{n-1} g_k s^k, \quad (8)$$

$$h(s) = \sum_{k=0}^{n-1} h_k s^k. \quad (9)$$

Substituting the Eq. (7) into the Eq. (6) leads to

$$X(s) = \frac{g(s)}{s^2 g(s) + b_0 h(s)} d_0 F_d(s). \quad (10)$$

The disturbance is assumed to be stepwise so that it can be modeled as

$$F_d(s) = \frac{F_0}{s} \quad (F_0: \text{const}). \quad (11)$$

The control parameters are selected so that to stabilize the closed loop system. Thus the steady-state displacement $x(\infty)$ could be stated by considering the Eqs. (10) and (11) as follows

$$\frac{x(\infty)}{F_0} = \lim_{s \rightarrow 0} \frac{g(s)}{s^2 g(s) + b_0 h(s)} d_0 = \frac{d_0 g_0}{b_0 h_0}. \quad (12)$$

If the system has stiffness of magnitude k_x , then ratio of steady state displacement and load can be defined as

$$\frac{x(\infty)}{F_0} = \frac{d_0 g_0}{b_0 h_0} = \frac{1}{k_x}. \quad (13)$$

For getting positive and negative stiffness, the value of k_x in designing the controller is selected as positive and negative value, respectively. Moreover, the infinite stiffness is acquired by considering the equal absolute value of k_x in

designing the both controllers which is shown in Fig. 4.

To assign the closed-loop poles arbitrarily, second or more-order compensator is necessary. When third-order compensator is considered, the characteristic polynomial of the closed-loop system (10) becomes 5th-order defined as follows

$$t_c(s) = s^5 + (g_2)s^4 + (g_1)s^3 + (g_0 + b_0h_2)s^2 + (b_0h_1)s + b_0h_0 \quad (14)$$

The characteristics polynomial of the 5th-order ideal system can be represented as follows

$$t_d(s) = (s^2 + 2\zeta_1\omega_1s + \omega_1^2)(s^2 + 2\zeta_2\omega_2s + \omega_2^2)(s + \omega_3) \quad (15)$$

$$= s^5 + e_4s^4 + e_3s^3 + e_2s^2 + e_1s + e_0.$$

The coefficients of the transfer function of the negative stiffness control system are determined uniquely by comparing the Eqs. (15) and (16) and using the condition of the Eq. (14). Finally, the controller gains become as follows

$$g_0 = \frac{e_0}{d_0k_n}, \quad (16)$$

$$g_1 = e_3, \quad (17)$$

$$g_2 = e_4, \quad (18)$$

$$h_0 = \frac{e_0}{b_0}, \quad (19)$$

$$h_1 = \frac{e_1}{b_0}, \quad (20)$$

$$h_2 = \frac{1}{b_0}(e_2 - g_0). \quad (21)$$

The developed active system (Fig. 5) consists of isolation table and middle mass (table). Both tables are vertically supported respect to base using free bearing. In the designing

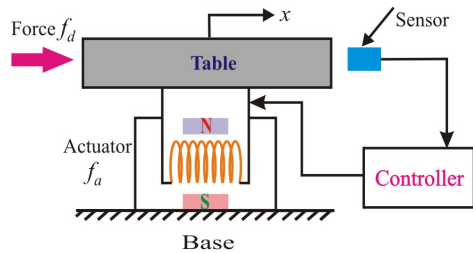


Fig. 3. Basic model of single axis active system

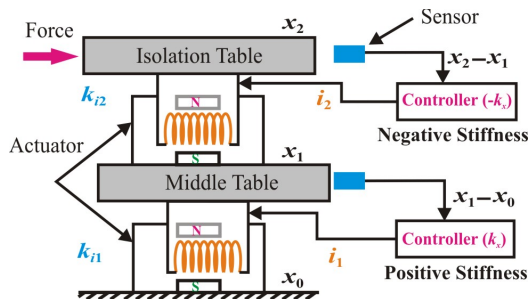


Fig. 4. Arrangement of the proposed control technique

of controllers of the developed system with negative stiffness control technique [4], the influences of the frictional effect are neglected. However, in actual circumstances, friction occurs in between the two moving mated parts of active or passive system. Thus the developed system encounters friction and consequently the system's performance deteriorates sufficiently. In the following sections, the induced friction and its consequent effects on the developed system with negative stiffness control are analyzed.

IV. DESCRIBING FUNCTION AND CORRESPONDING LIMIT CYCLE

The describing function is one of the useful tools to analyze the nonlinearity of nonlinear control system. The describing function of a nonlinear element is defined as the complex ratio of the Fourier series fundamental component of the output to a sinusoidal input [6].

Let us consider a feedback control system consists of linear and nonlinear parts shown in Fig. 6. The open loop transfer functions of linear and nonlinear parts of the system are denoted by $G(s)$ and $TF_n(x_0, \omega)$, respectively. To define the nonlinearity by describing function, the sinusoidal input to nonlinear part is considered as

$$x(t) = x_0 \sin(\omega t). \quad (22)$$

The output of the nonlinear part $y(t)$ is not obviously sinusoidal but periodic with same period of input. The output contains higher order harmonic of the fundamental component. If the behavior of the accomplished nonlinearity is symmetry respect to around zero response, then its periodic output could be expanded by a Fourier series as follows [6]

$$y(t) = \sum_{n=0}^{\infty} a_n \cos n\omega t + b_n \sin n\omega t, \quad (23)$$

where

$$a_n = \frac{1}{\pi} \int_0^{2\pi} y(t) \cos(n\omega t) d(\omega t), \quad b_n = \frac{1}{\pi} \int_0^{2\pi} y(t) \sin(n\omega t) d(\omega t).$$

The fundamental (first) harmonic of the output is usually considered to find the describing function [7] as higher-order

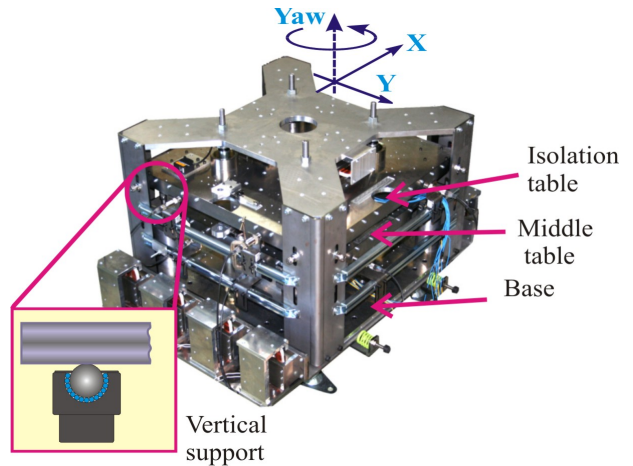


Fig. 5. Photograph of developed active system

components are smaller in magnitude and the low pass filter in the control system further attenuates the higher harmonics. Thus the describing function (D) of the nonlinearity corresponds to the Eqs. (23) and (24) becomes as follows

$$D = \frac{y_1(t)}{x(t)} = \frac{a_1 \cos \omega t + b_1 \sin \omega t}{x_0 \sin \omega t} \quad (24)$$

If the input and output of the nonlinearity are the respective desired input and output of the nonlinear part, then the Laplace-transform of the corresponding describing function represents the nonlinear part (TF_n) shown in below

$$TF_n(x_0, \omega) = L[D] = \frac{L[y_1(t)]}{L[x(t)]} = \frac{L[a_1 \cos \omega t + b_1 \sin \omega t]}{L[x_0 \sin \omega t]} \quad (25)$$

$$= \frac{a_1 \frac{s}{s^2 + \omega^2} + b_1 \frac{\omega}{s^2 + \omega^2}}{x_0 \frac{\omega}{s^2 + \omega^2}} \Bigg|_{s=j\omega} = \frac{a_1 j + b_1}{x_0}$$

The close-loop transfer function of the whole nonlinear control system shown in Fig. 6 can be expressed as

$$\frac{Q(j\omega)}{R(j\omega)} = \frac{TF_n(x_0, \omega)G(j\omega)}{1 + TF_n(x_0, \omega)G(j\omega)} \quad (26)$$

The characteristic polynomial of the respective close-loop nonlinear control system (Fig. 6) is defined by

$$1 + TF_n(x_0, \omega)G(j\omega) = 0 \quad (27)$$

$$G(j\omega) = -\frac{1}{TF_n(x_0, \omega)}$$

The characteristics polynomial (27) consists of open loop transfer function of linear and nonlinear parts. Thus the limit cycle will appear in the control system if the Eq. (27) is satisfied for parameters in nonlinear part (x_0 and ω) [8]. Since $G(j\omega)$ and $TF_n(x_0, \omega)$ are complex function of x_0 and ω so the solution of the Eq. (27) gives both the frequency and amplitude of the limit cycle (self-oscillation).

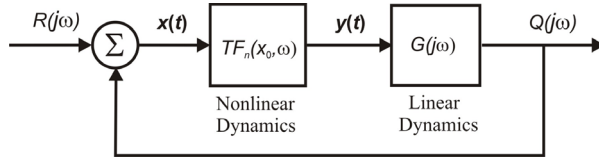


Fig. 6. Feedback control system with nonlinearity

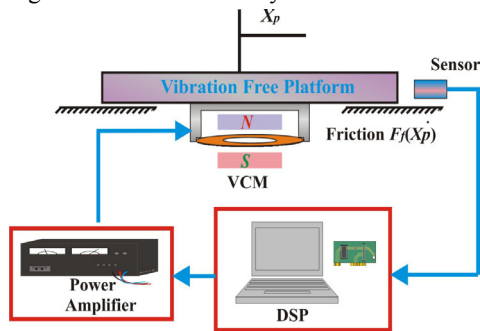


Fig. 7. Schematic diagram of developed active system

V. DESCRIPTION OF DEVELOPED SYSTEM WITH FRICTION NONLINEARITY

The self-oscillation of a nonlinear system can be analyzed by its close loop characteristics equation [8]. However, for such analysis, the characteristic equation has to be defined with its open loop transfer function of linear and nonlinear part together. Hence to analyze the limit-cycle of the developed system, the defining of its linear and nonlinear parts are explored in this section. The simplified block diagram of the developed system with negative stiffness control is shown in Fig. 8. The ultimate open loop transfer function representation of the whole system dynamics respect to displacement and reference input is given by

$$G_c(s) = \frac{X_p(s)}{X_d(s)} = \frac{k_i G_n(s)}{ms^2 + D_f s} \quad (28)$$

where

$G_n(s)$: stiffness controller transfer function

D_f : describing function of friction nonlinearity

x_p, x_d : table displacement and reference input, respectively.

Since the open loop transfer function of the whole system $G_c(s)$ includes the linear and the nonlinear part dynamics, therefore it could be also presented by

$$G_c(s) = G(s)N(x_0, \omega) \quad (29)$$

where

$G(s)$: linear part open loop transfer function

$N(x_0, \omega)$: nonlinear part open loop transfer function.

The nonlinearity is assumed in the control system due to friction only. Therefore when friction is cancelled ($D_f = 0$) then open loop transfer function of the whole system turns into the open loop transfer function of linear part. It means that, the linear part of the system consists of controller, actuator and table. Hence corresponding open loop frequency response of linear part is presented as

$$G(s) = \frac{k_i G_n(s)}{ms^2} \quad (30)$$

Once the open loop transfer function of the linear part is obtained then nonlinear part can be determined as

$$N(x_0, \omega) = \frac{G_c(s)}{G(s)} = \frac{ms^2}{ms^2 + D_f s} \quad (31)$$

The negative inverse of the nonlinear part in the control system can be presented as below

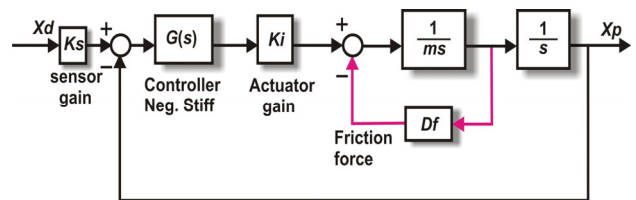


Fig. 8. Simplified block diagram for linear and nonlinear part of negative stiffness control developed system

$$-\frac{1}{N(x_0, \omega)} = -\frac{ms^2 + D_f s}{ms^2} = -1 + j \frac{D_f}{m\omega}. \quad (32)$$

A. Describing function of friction

The nonlinear coulomb friction and stibeck effects arise at low velocity region but at higher velocity region, little viscous resistance takes place [5]. In the developed system, contact areas between table and vertical supports are grease lubricated. So the viscous effect is neglected in this study as it causes very minor effect in total induced friction. Therefore the friction for the developed system can be modeled as shown in Fig.9. Before starting of motion, the surface is static region and intuitively, a force greater than the static friction (F_s) is required to move and friction suddenly decreases when table starts to move. Usually the friction nonlinearity takes place around zero velocity of the system. Therefore the constant friction force over the higher velocity region is kept in the proposed friction model. The higher velocity region is assumed beyond the velocity V_0 which corresponds to zero static friction and zero stibeck effect in the applied friction model (Fig. 9).

The output behavior of the nonlinear friction respect to sinusoidal input is determined by describing function of the nonlinear friction (D_f) of the developed system. The sinusoidal input to the nonlinear developed system is considered as follows

$$x(t) = V_m \sin(\omega t), \quad (33)$$

where V_m and ω are maximum amplitude and frequency of input sinusoidal velocity, respectively. Then the applied friction model shown in Fig. 13 could be expressed mathematically as follows

$$F_f(t) = \begin{cases} F_c + F_s - K_1 V_m \sin(\omega t) & 0 < t < t_1 \\ F_c & t_1 < t < \frac{\pi}{\omega} - t_1 \\ F_c + K_1 V_m \sin(\omega t) & \frac{\pi}{\omega} - t_1 < t < \frac{\pi}{\omega} \end{cases}, \quad (34)$$

where

$$t_1 = \frac{1}{\omega} \sin^{-1} \left(\frac{V_0}{V_m} \right)$$

K_1 : viscous coefficient at low velocity region.

The Fourier series output expression of periodic induced friction ($F_f(t)$) can be written as

$$F_f(t) = \sum_{n=0}^{n=\infty} (a_n \cos n\omega t + b_n \sin n\omega t). \quad (35)$$

Since $F_f(t)$ is an odd function, so it contains only sine term. Therefore the first harmonic output of the nonlinear friction could be expressed by Fourier series as follows [7]

$$F_{f1}(t) = b_1 \sin \omega t, \quad (36)$$

where

$$b_1 = \frac{1}{\pi} \int_0^{2\pi} F_f(t) \sin(\omega t) d(\omega t) = \frac{2\omega}{\pi} \int_0^{\pi/\omega} F_f(t) \sin(\omega t) dt. \quad (37)$$

Substituting the Eq. (34) into the Eq. (37) with considering the Eq. (36) leads the first harmonic output given in below

$$F_{f1}(t) = \frac{2}{\pi} \left[2F_c + F_s - F_s \cos \left\{ \sin^{-1} \left(\frac{V_0}{V_m} \right) \right\} \right] \sin(\omega t). \quad (38)$$

Hence the sinusoidal input describing function of the friction [$D_f(V_m, V_0)$] to the developed can be defined as follows

$$D_f(V_m, V_0) = \frac{2}{\pi V_m} \left[2F_c + F_s - F_s \cos \left\{ \sin^{-1} \left(\frac{V_0}{V_m} \right) \right\} \right]. \quad (39)$$

B. Limit cycle prediction

The response of the close loop control developed system respect to reference input can be expressed as

$$\frac{X_p(s)}{X_d(s)} = \frac{G(s)N(V_m, \omega)}{1 + G(s)N(V_m, \omega)}, \quad (40)$$

where $G(s)$ and $N(x_0, \omega)$ are open loop transfer function of the linear and nonlinear part in the developed system, respectively. The procedures to determine the open loop transfer function of the linear and nonlinear parts of the negative stiffness control developed system are mentioned in earlier (Eqs. (30) and (31)). The characteristic equation of the close loop negative stiffness control developed system is defined by

$$1 + G(s)N(V_m, \omega) = 0 \Rightarrow G(s) = -\frac{1}{N(V_m, \omega)}. \quad (41)$$

Thus the limit cycle would be able to sustain in the developed system if any condition of nonlinearity satisfies the Eq. (41). In other words, a self-excited oscillation exists with amplitude V_m and frequency ω when a proper selection of $h(s)$ and $g(s)$ satisfies the Eq. (41).

VI. RESULT AND DISCUSSION

The Nyquist plot approach is conducted to find the existence of limit cycle in the negative stiffness control developed system theoretically. The Nyquist curves of linear and negative inverse nonlinear parts are drawn together on same complex plane shown in Fig. 10. The intersection of the Nyquist curves represents the existence of limit cycle. In this analysis the limit cycles are distinguished for different magnitude of negative stiffness k_x varied (Eq. 13) from -20 to

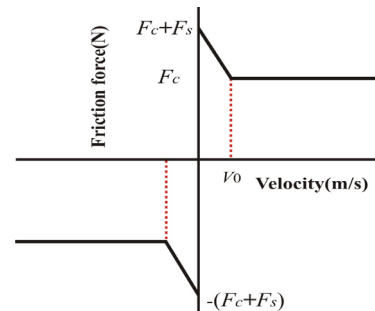


Fig. 9. Applied friction model

-35 N/mm. Here it is observed that the frequency of induced limit cycle is higher for low negative stiffness compared to that of higher negative stiffness.

However the linear part of the positive stiffness ($k_x = 25$ N/mm) control system does not intersect the nonlinear part shown in Fig. 11. Thus positive stiffness control system is free from the effects of limit cycle. Moreover the nonlinear parts in both positive stiffness and negative stiffness control are determined for same conditions.

The experimental analyses are carried out to verify the limit cycle obtained theoretically in the Figs. 10 and 11. Experimental time responses to self-oscillation for different magnitudes of negative stiffness (same as Fig. 10) are drawn in Fig. 12. The negative stiffness are selected as -20 N/mm, -25 N/mm, -30 N/mm, -35 N/mm and corresponding self-oscillation frequencies are observed around 0.35Hz, 0.25Hz, 0.2Hz and 0.14 Hz, respectively which sufficiently satisfy the theoretical results shown in Fig. 10. Hence theoretical limit cycles of a specific negative stiffness control system for several sets of control parameters will assist to predict the actual limit cycle of that system.

VII. CONCLUSIONS

The horizontal vibration isolation table with negative stiffness control behaves self-oscillation. The frequency of the limit cycle (self-oscillation) is inversely proportional to the magnitude of negative stiffness of the control system. The friction nonlinearity is mainly responsible for such instability in the negative stiffness control developed system. Meanwhile, the same system with the positive stiffness control is unaffected by such nonlinearity as well as it is free from limit cycle. The compensating of nonlinearity as well as reduction of limit cycle from negative stiffness control system will be conducted in future work.

ACKNOWLEDGMENT

The authors would like to acknowledge the financial

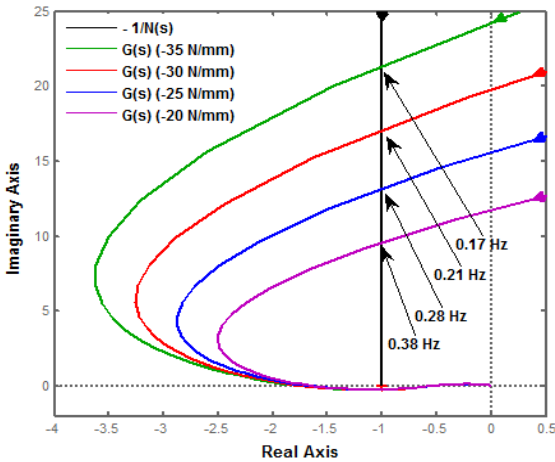


Fig. 10. Limit cycle for different magnitude of negative stiffness

support received from the Ministry of Education, Culture, Sports, Science and Technology of Japan in part as a Grant-in-Aid for Scientific Research (B).

REFERENCES

- [1] Rivin, E. I., *Passive Vibration Isolation*, ASME Press, New York, (2003).
- [2] Mizuno, T., Takasaki, M., Kishita, D., and Hirakawa, K., "Vibration Isolation System Combining Zero-Power Magnetic Suspension With Springs", *Control Engineering Practice*, vol. 15, no. 2, pp. 187-196, 2006.
- [3] Mizuno, T., Toumiya, T. and Takasaki, M., "Vibration Isolation Using Negative Stiffness," *JSME International Journal*, Series C, vol. 46, (3), pp. 807-812, 2003.
- [4] Shahadat, M. M. Z., Mizuno, T., Ishino, Y., and Takasaki, M., "Active Horizontal Suspension Using Negative Stiffness Control," *International Conference on Control, Automation and System 2010*, KINTEX, Gyeonggi-do, Korea, Oct 27-30, 2010.
- [5] Yuan-Jay, W., "Characterization and quenching of friction-induced limit cycles of electro-hydraulic servo valve control system with transport delay," *ISA Transactions*, vol. 49 (2010), pp. 489-500, 2010.
- [6] Atherton, D. P., *Nonlinear control engineering*, 77. J. W. Arrowsmith Ltd., Great Britain, 1975.
- [7] Kolk, W. R., Lerman, R. A., *Nonlinear system dynamics*, 95. Van Nostrand Reinhold, New York, 1992.
- [8] F. B. Duarte, J. T. Machado, "Fractional Describing Function of Systems with Coulomb Friction," *Nonlinear Dyn*, vol. 56, pp. 381-387, 2009.

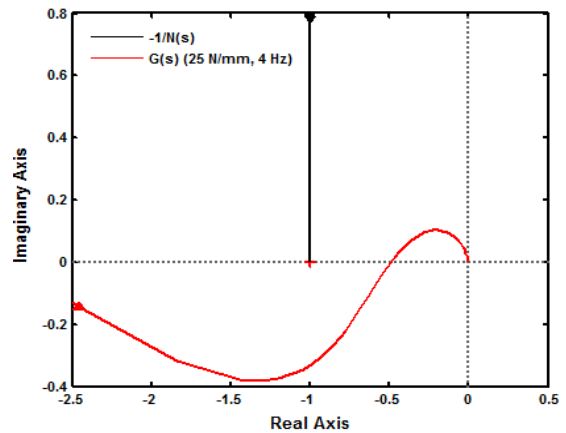


Fig. 11. Nyquist plot positive stiffness control system

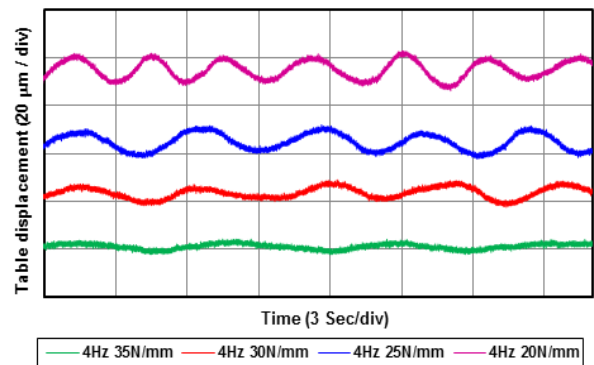


Fig. 12. Time response to Self-oscillation at different magnitude of negative stiffness